NASA TECHNICAL NOTE

NASA TN D-1976

NASA TN D-1976

MOMENTUM ACCOMMODATION OF N^+, N_2^+, AND A^+ INCIDENT ON COPPER AND ALUMINUM FROM 0.5 TO 4 KEV

by Howard F. Savage and Michel Bader

Ames Research Center

Moffett Field, California

NATIONAL AERONAUTICS AND SPACE ADMINISTRATION • WASHINGTON, D. C. • SEPTEMBER 1963

TECHNICAL NOTE D-1976

MOMENTUM ACCOMMODATION OF N^+, N_2^+, AND A^+ INCIDENT ON COPPER AND ALUMINUM FROM 0.5 TO 4 KEV

By Howard F. Savage and Michel Bader

Ames Research Center
Moffett Field, California

NATIONAL AERONAUTICS AND SPACE ADMINISTRATION

NATIONAL AERONAUTICS AND SPACE ADMINISTRATION

TECHNICAL NOTE D-1976

MOMENTUM ACCOMMODATION OF N^+, N_2^+, AND A^+ INCIDENT ON COPPER AND ALUMINUM FROM 0.5 TO 4 KEV

By Howard F. Savage and Michel Bader

SUMMARY

The normal and tangential components of the force due to ion (N^+, N_2^+, or A^+) bombardment of a flat plate (Cu or Al) have been measured with a two-component microbalance. The forces were measured for ion energies between 0.5 and 4.0 kev at angles of incidence from 0 to 50° from the normal. The normal and tangential momentum accommodation coefficients computed from these measurements range generally from 0.3 to 0.9. It is suggested, on the basis of these and available sputtering yield and distribution data, that the departures from complete accommodation are due primarily to the ejection of target atoms.

INTRODUCTION

At sufficiently low densities, the molecular mean free path in a gaseous medium becomes much larger than the dimensions of any given body immersed in the gas. This is the free molecule flow regime which has received increased attention lately because of problems of flight in rarefied media at satellite and higher velocities. Under these conditions, molecule-molecule collisions are negligible compared to molecule-surface collisions, and the interactions between the individual impinging gas molecules and the solid surface determine the forces exerted on the body. Most of the published experimental work to date has been concerned almost exclusively with the transfer of energy between the gas and the solid surface (thermal accommodation coefficients) at less than 1 ev incident energy. This experimental work has been summarized by Wachman (ref. 1) and Hartnett (ref. 2). Very little data are, however, available, particularly on the transfer of momentum from the impinging gas molecules to the solid (momentum accommodation coefficients), for conditions characteristic of earth satellites and space vehicles, that is, for combinations of gases such as atomic and molecular nitrogen and oxygen and engineering materials like aluminum, with relative velocities equal to and greater than earth satellite velocities (energies in excess of 10 ev). The objectives of the present investigation were, therefore, to provide experimental data on and to gain some understanding of the details of the momentum transfer from high velocity ion beams to some of the metallic surfaces of interest. Thermal accommodation coefficients could not be derived from the experiments performed because of complications introduced by the ejection of surface material (sputtering).

SYMBOLS

A	area of condenser plate
d	condenser plate separation
F	force between plates of a condenser
F_n, F_t	normal and tangential components of force per unit area
p_i	normal component of incident momentum
p_r	normal component of recoil momentum (momentum imparted to the target by the reflection and/or emission of particles)
p_w	normal component of recoil momentum for complete accommodation
T_i, T_r, T_w	incident, reflected, and wall thermal energies
ΔV	voltage across condenser plates
α	energy accommodation coefficient
θ	angle measured from normal
σ_n, σ_t	normal and tangential accommodation coefficients
τ_i	tangential component of incident momentum
τ_r	tangential component of recoil momentum (momentum imparted to the target by the reflection and/or emission of particles)

THE ACCOMMODATION COEFFICIENTS

It has been found convenient to study energy and momentum transfer to a body in free molecule flow in terms of accommodation coefficients. The energy accommodation coefficient, α, is defined by:

$$\alpha = \frac{T_i - T_r}{T_i - T_w} \tag{1}$$

where T_i is the incident beam energy, T_r is the reflected energy, and T_w is the wall temperature multiplied by Boltzmann's constant.

There are two momentum accommodation coefficients, σ_n and σ_t, for the normal and for the tangential components of momentum,

$$\sigma_n = \frac{p_i - p_r}{p_i - p_w} \tag{2a}$$

$$\sigma_t = \frac{\tau_i - \tau_r}{\tau_i} \tag{2b}$$

where p and τ are, respectively, the magnitudes of the normal and tangential components of momentum per unit area per unit time. The subscripts i and r denote incident and reflected conditions. The term p_w is the normal momentum component that the reflected beam would have if it were re-emitted with a Maxwellian velocity distribution corresponding to the surface temperature. For the range of p_i of the present investigation, $p_w \ll p_i$ and can be considered to be zero. The analogous term τ_w is zero by symmetry.

In the experiments herein reported, the incident momentum was known and the normal and tangential components of force, F_n and F_t, were measured. In terms of these parameters (see fig. 1),

$$\sigma_n = 1 - \frac{p_r}{p_i} = 1 - \frac{F_n - p_i}{p_i} = 2 - \frac{F_n}{p_i} \tag{3a}$$

$$\sigma_t = 1 - \frac{\tau_r}{\tau_i} = 1 - \frac{\tau_i - F_t}{\tau_i} = \frac{F_t}{\tau_i} \tag{3b}$$

Equations (3) give the basis for determining the momentum accommodation coefficients. The energy accommodation coefficient, α, on the other hand, cannot be determined from force measurements unless the angular and velocity distributions of particles ejected from the surface are known. The picture is further complicated when the energy of the incident particles exceeds the sputtering

threshold, since then the ejected particles include both reflected or re-emitted beam particles and surface material. It is important, under these conditions, to differentiate carefully between accommodation of the incident momentum and energy, as defined by equations (1) to (3), and accommodation of the incident beam, which means thermalization and re-emission in random directions of the incident particles.

APPARATUS

Normal and tangential forces were measured by letting an ion beam impinge on flat targets mounted on a microbalance in the ion accelerator vacuum system.

The Ion Accelerator

The accelerator has been described in detail by Bader, Witteborn, and Snouse (ref. 3) so that only a brief outline of the essentials will be given. The ions are extracted from an rf source, electrostatically focused into a magnetic analyzer to separate the desired ions from any others, then electrostatically focused onto the target. Beam energy variations are obtained by changing the ion extraction voltage and/or the target potential. The energy is measured by making retarding potential measurements at the target. The energy dispersion in the beam is typically about 40 ev.

The Microbalance

The two-component microbalance constructed for measuring the forces on flat plates in free molecule flow has been described in detail by Rogallo and Savage (ref. 4). Details of the balance suspension, electrode system, and housing are shown in figures 2 and 3. Briefly, the balance is a null reading instrument in which the electrostatic attraction between parallel plates is used to balance the components of force due to the ion bombardment of the flat plate target. Two perpendicular pairs of plates are used to measure, respectively, the normal and tangential components of the force. The movable part of the system is essentially a pendulum with the center of gravity very slightly below the point of suspension.

The forces are calculated from the plate area A, separation d, and potential difference ΔV in accordance with the relation:

$$F \text{ (dynes)} = \frac{10^{-4}}{72\pi} \frac{A(\Delta V)^2}{d^2}$$

For the present system, A = 545 mm^2, and d = 3.14 mm, which leads to the relation:

$$F \text{ (micrograms)} = 2.49 \times 10^{-2} (\Delta V)^2$$

The sensitivity of the balance is adjusted by changing the mass of the control weight (fig. 2). For the greatest usable sensitivity, the balance is capable of detecting tangential forces of 2 to 3 micrograms and normal forces of 4 to 5 micrograms. Greater sensitivities can be achieved but, as the point of instability is approached, it becomes very difficult and tedious to make a force measurement.

TEST PROCEDURE

The metal targets, Cu (cold rolled sheet) or Al (2024 Alclad Soft), were each 1-1/8 inches in diameter and had a mass of approximately 1.5 grams. The targets were cleaned and polished before being positioned on the balance, but, because of the long time (several hours) necessary to adjust the balance, the surfaces were subject to some atmospheric contamination. Before each series of data points were recorded, the ion beam was focused on the target for several minutes to sputter away possible contaminants and also to reduce a zero shift which frequently occurred in the normal force at high ion energies. The cause of this shift is not certain. It is believed to be related to the heating of the target material since it occurred most frequently at high beam powers, was always in the same direction, and did not appear in the tangential force (the geometry of the balance is such that a target thermal distortion would affect only the normal force measurement).

The true ion current could not be measured at the target because the balance was greatly disturbed by the potential necessary to suppress secondary electrons. The following procedure was therefore followed. The ion beam was focused on the target by monitoring the unsuppressed current. This current was then compared to the unsuppressed current to a probe which was of the same material as the target and was located 1.5 inches ahead of the target. The secondary electron current to the probe was then suppressed to measure the true ion current to the probe from which the target ion current could be computed. Ion currents of 10 to 60μa were used, depending upon the ion and ion energy. The beam was focused on a 3/8-inch-diameter area centered on the target.

Forces in μg/μa were computed from the ion beam current and the potential differences which had to be applied to the capacitor plates to obtain a null reading of the balance. The measured forces ranged from 15 to 250μg for the normal force and from 6 to 70μg for the tangential force.

The pressure in the target chamber, as measured by an ionization gage, ranged between 1.8 and 5.0×10^{-6} torr during the measurements (typically 2.5×10^{-6} torr). The background pressure was near 8×10^{-7} torr.

RESULTS

Typical force data for Cu and Al bombarded by N_2^+ are presented in figure 4. Each point on the graph is an average of 3 to 6 measurements. The scatter in these averages is typical of the scatter in the raw data. Also shown are the curves which would result from zero and complete momentum accommodation. As one might expect, the data lie between these two extremes.

Since momentum accommodation coefficients are more convenient than forces for analysis and comparison, these computed data are presented in detail in figures 5 through 8. The values of σ_n and σ_t as functions of angle of incidence for the ion-target configurations studied are given in figures 5 through 7 at two energies for each combination. Both σ_n and σ_t decrease as the angle of incidence departs from the normal for all ion-target combinations tested. The decrease in σ_n is greater than that of σ_t in most cases. The decrease in σ_n was greater for A^+ on both Cu and Al than for N_2^+ or N^+ and the decrease in σ_n was greater for Cu than for Al. Both σ_n and σ_t are greater for Al than for Cu when bombarded by the same ion at the same energy and angle of incidence. Both σ_n and σ_t are less over the range of angles of incidence for A^+ on Cu than for N_2^+ or N^+, but there are only slight differences in the case of Al.

The values of σ_n as a function of energy for the ion at normal incidence are shown in figure 8. For the range of test conditions, the variations with ion energy are smaller than the more prominent of the variations with angle of incidence.

DISCUSSION

Since the bombarding energies considered in this report are well in excess of sputtering thresholds (ref. 3), it is to be expected that ejected surface material as well as reflected beam particles contributed to the measured forces. It behooves us, therefore, to review briefly what is known about the angular and velocity distributions of reflected and sputtered particles.

The angular distribution of reflected beam particles is poorly known, especially at the incident energies considered in the present report. There are strong arguments as follows, however, to indicate that the incident beam should be fully accommodated, so that the reflected beam intensity in a given direction is proportional to the cosine of the angle θ from the normal (fig. 9). From quantum mechanical considerations, one would expect specular reflection or diffraction effects only when the de Broglie wavelength of the incident particles is comparable with lattice dimensions. This condition is approached only for the lightest elements at energies under 1 ev (the de Broglie wavelength of a 1 ev proton is 3×10^{-9} cm). At higher energies and for larger masses, one can see qualitatively that the incident particle penetrates deeper and is less likely

to be reflected as its mass increases. In particular, polyatomic incident molecules can be expected to break up on impact, so that specular reflection cannot occur. These trends have been experimentally verified at thermal energies by Stickney (ref. 5).

The distribution of atoms sputtered from polycrystalline targets differs from the cosine and depends upon the incident ion energy. At normal incidence, ions with energies less than about 1 kev may produce an under cosine distribution (fig. 9), as reported, for example, by Wehner and Rosenberg (ref. 6), while the sputtered atoms from 20 kev incident ions may have an over cosine distribution as reported, for example, by Perović and Cobić (ref. 7). At angles of incidence other than normal, the sputtered atoms may be ejected with a distribution skewed in a forward direction, as shown on figure 10 (unpublished data obtained by T. W. Snouse, Ames Research Center).

The velocities of sputtered atoms have been measured by Wehner (refs. 8 and 9) for a few combinations of ions and metals (fig. 11). The corresponding energies are of the order of 10 to 30 ev for atoms sputtered by normally incident Hg^+ ions at 0.1 to 1 kev.

At the bombarding energies considered in this report, one may assume, then, that the momentum of the reflected beam particles is negligible compared to that of the sputtered material: the energy of the reflected particles is probably 100 to 1000 times less, and their actual numbers are 1 to 5 times smaller (ref. 3) than those of sputtered particles. At normal bombarding incidence, one may furthermore assume a nearly cosine mass distribution for the sputtered material. In the following discussion, we shall attempt to show that the measured accommodation coefficients are consistent with the above assumptions and existing sputtering data.

As a first correlation, one may compute from the accommodation data and known sputtering yields (ref. 3) an average velocity of the sputtered material which would be consistent with the forces measured experimentally. These velocities, as shown in figure 11, are of the same magnitudes as were measured by Wehner (ref. 9) in the case of Ni and W bombarded by Hg^+, and also as calculated (ref. 8) for Cu - Hg^+.

Another interesting result is shown on figure 10, where the center of mass of the ejected material is indicated as well as the direction of the reflected momentum as computed from the force measurements. Since φ momentum $> \varphi$ mass, it must be that the velocities of sputtered atoms are larger in the forward direction. This effect has been observed in the few isolated cases for which data are available (ref. 9).

The observed dependence of the accommodation coefficients on the angle of incidence (figs. 5 through 7) indicates that sputtering is the main determining factor for these variations. As one can see from figure 10, the distribution of sputtered material is skewed in the direction of specular reflection. It is known also that the sputtering rate increases with the angle of incidence (ref. 3). This increase in the sputtering rate can account for the large decrease in σ_n, while the deviation from the cosine distribution of the sputtered material can

account for the decrease in σ_t (figs. 5 and 6). The lower sputtering yield of Al accounts for the accommodation coefficients being higher for Al than for Cu. The lobe toward the forward direction (fig. 10) becomes slightly more pronounced as the energy is decreased (T. W. Snouse, unpublished data) and, therefore, σ_t should decrease more with increasing angle of incidence at the lower energies. There is a definite trend in this direction as can be seen, for example, by comparing σ_t at 1080 ev and at 2060 ev for N_2^+ on Cu (fig. 5).

The effects on momentum accommodation of the relative masses of the bombarding ion and of the target atoms may be analyzed for the following three cases. We may compare, first, bombardment by atomic and molecular ions of the same species; second, bombardment of different targets by a given ion; and, third, bombardment of a given target by different ions.

In the absence of sputtering, and if equal amounts of incident momentum are equally accommodated, then one would expect N^+ to exhibit the same coefficients as N_2^+ at half the energy. This is not the case for the data on figure 5. On the other hand, again ignoring sputtering, since the incident N_2^+ probably dissociates on impact (dissociation energy = 9.76 ev) into two atoms of about equal energy,[1] one would expect the accommodation coefficients to be the same for N^+ as for N_2^+ at twice the energy. This is not the case either, as can be seen from the data on figure 8. These negative results are, of course, what one would expect if sputtering is important (see ref. 3).

The accommodation coefficients for a given ion are lower for Cu than for Al (figs. 5 and 6). This is consistent with the higher sputtering rate of Cu than Al (ref. 9).

The accommodation coefficients of N^+, N_2^+, and A^+ on Cu decrease in the order mentioned (fig. 7(a)). This is consistent with the increase of sputtering rates with mass in the energy range of interest (ref. 3). This effect is not apparent for the Al target (fig. 7(b)) except for the larger angles of incidence for which Al sputtering becomes appreciable.

In summary, then, the main features of the measured accommodation curves are consistent with the assumption that sputtering is a dominant factor at the energies herein considered. A more quantitative account must, therefore, await more complete data on sputtering distributions.

CONCLUDING REMARKS

It was shown in the discussion that simple momentum transfer from the beam particles to the targets does not explain the observed behavior of the accommodation coefficients, but that a qualitative understanding can be obtained by

---

[1]Supporting evidence has been given by Panin (ref. 10) who found that secondary ion energy spectra were the same for molecular incident ions and for monatomic incident ions of half the energy.

taking sputtering into account. It has also been made plausible from theoretical arguments that the incident particles are reflected in random directions with near-thermal (i.e., negligible) energies. The observed deviations from complete accommodation can therefore probably be attributed entirely to the ejection of sputtered material. A quantitative verification of this hypothesis is not possible without detailed data on velocity distributions of sputtered material, as well as similar data on reflected particles.

Ames Research Center
National Aeronautics and Space Administration
Moffett Field, Calif., May 13, 1963

REFERENCES

1. Wachman, H. Y.: The Thermal Accommodation Coefficient: A Critical Survey. American Rocket Society Journal, vol. 32, no. 1, Jan. 1962, pp. 2-12.

2. Hartnett, J. P.: A Survey of Thermal Accommodation Coefficients. Res. Memo. 2585, The Rand Corporation, March 19, 1960.

3. Bader, Michel, Witteborn, Fred C., and Snouse, Thomas W.: Sputtering of Metals by Mass-Analyzed N_2^+ and N^+. NASA TR R-105, 1961.

4. Rogallo, Vernon L., and Savage, Howard F.: Two-Component Microbalance for Measuring the Forces on Ion-Bombarded Surfaces. Review of Scientific Instruments, vol. 34, Sept. 1963.

5. Stickney, R. E.: An Experimental Investigation of Free Molecule Momentum Transfer Between Gases and Metallic Surfaces. U. of Calif. Tech. Rept. HE-150-182, Jan. 25, 1962.

6. Wehner, G. K., and Rosenberg, D.: Angular Distribution of Sputtered Material. Jour. Appl. Phys., vol. 31, no. 1, Jan. 1960, pp. 177-179.

7. Perović, B., and Cobić, B.: Cathode Sputtering of Cu and Ag by A^+ Ions of Energies from 10-200 keV. Proc. Fifth International Conf. on Ionization Phenomena in Gases, vol. II, 1962, pp. 1165-1171.

8. Wehner, G. K.: Forces on Ion-Bombarded Electrodes in a Low-Pressure Plasma. Jour. Appl. Phys., vol. 31, no. 8, Aug. 1960, pp. 1392-1396.

9. Wehner, G. K.: Velocities of Sputtered Atoms. The Physical Review, vol. 114, no. 5, June 1, 1959, pp. 1270-1272.

10. Panin, B. V.: Interaction of Medium-Energy (10-100 keV) Atomic Particles with Solids (Energy Spectra of Secondary Ions). Soviet Physics JETP, vol. 15, no. 2, Aug. 1962, pp. 215-221.

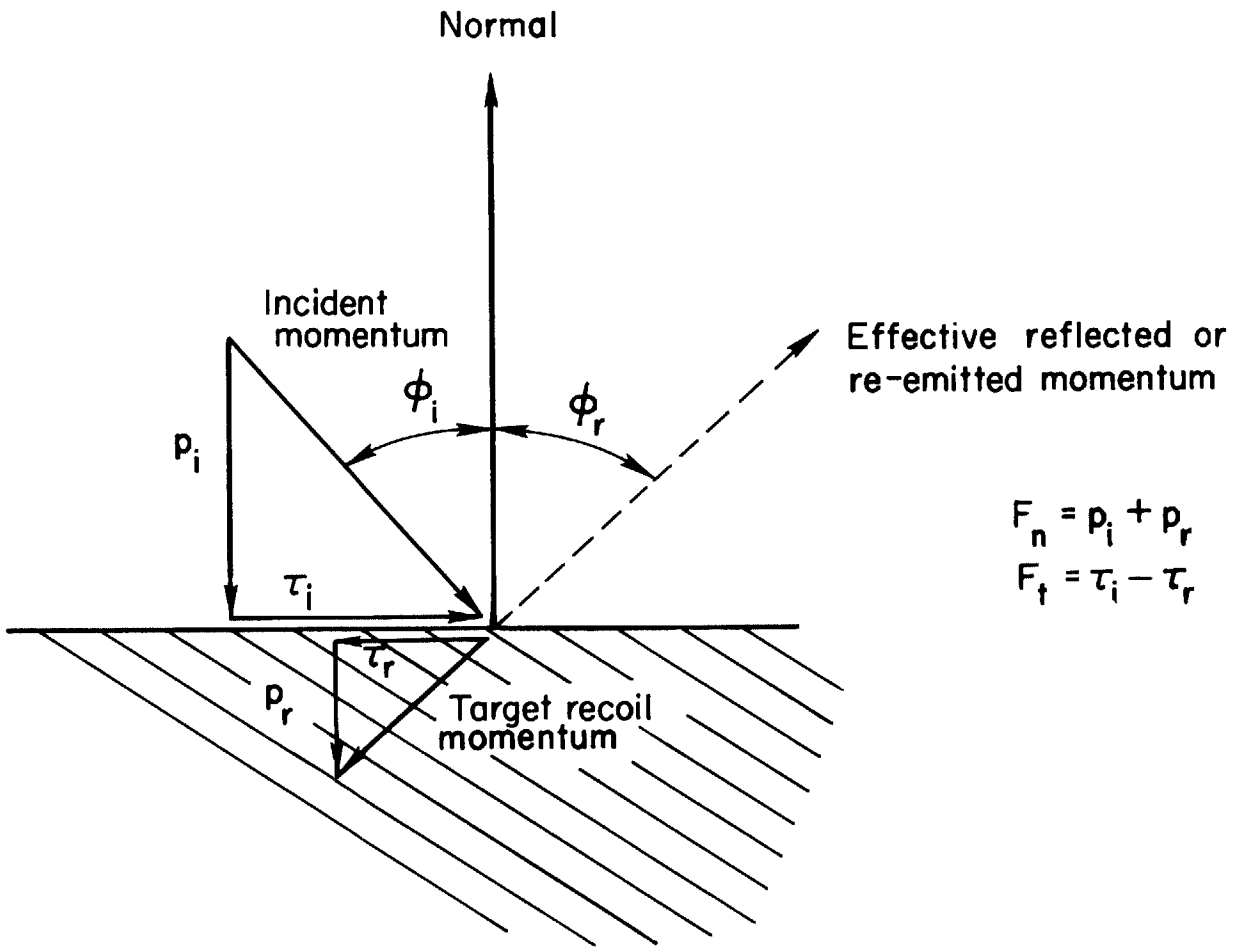

Figure 1.- Geometry and notation of the surface interaction.

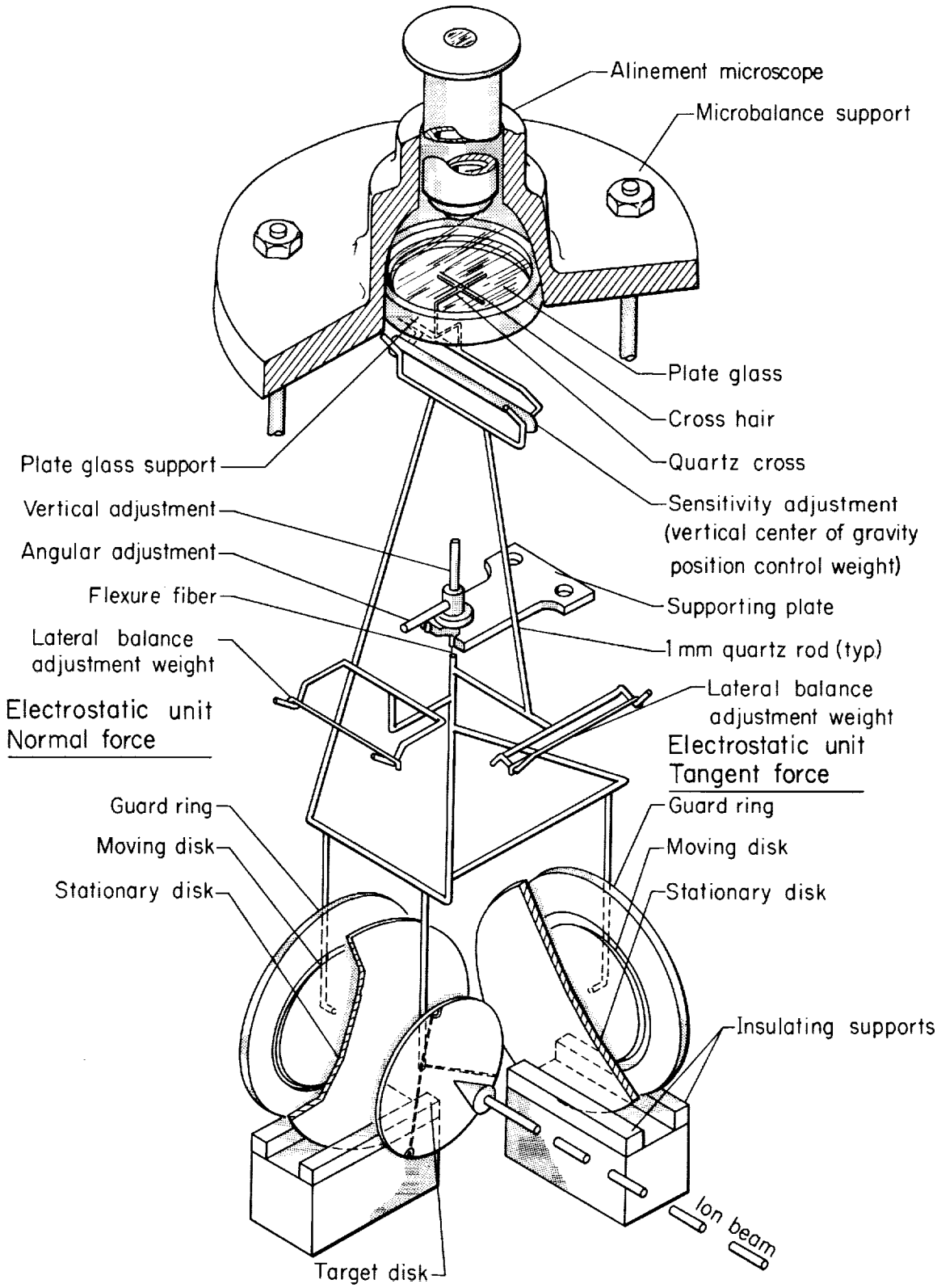

Figure 2.- Balance suspension and electrode systems.

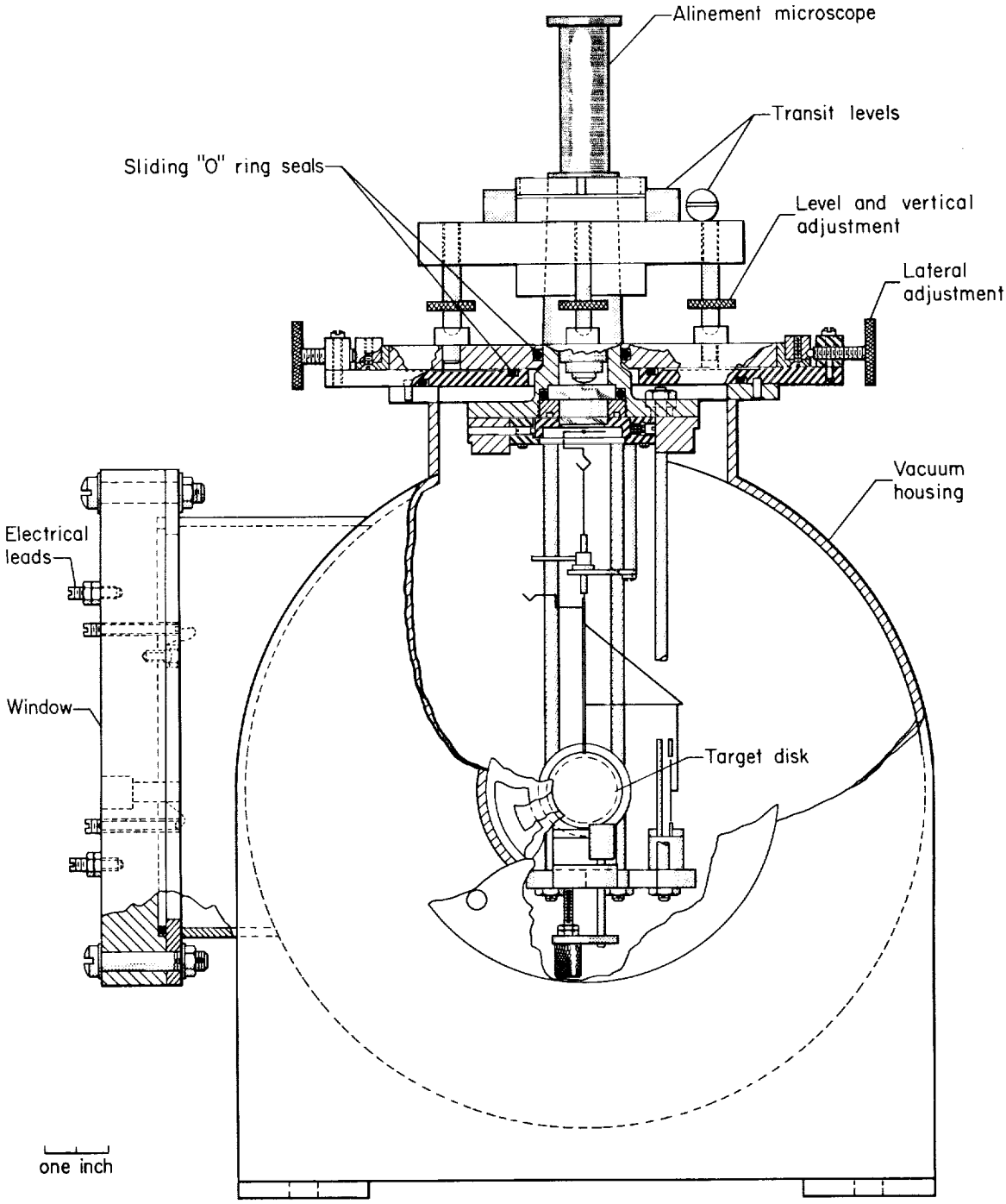

Figure 3.- Balance housing.

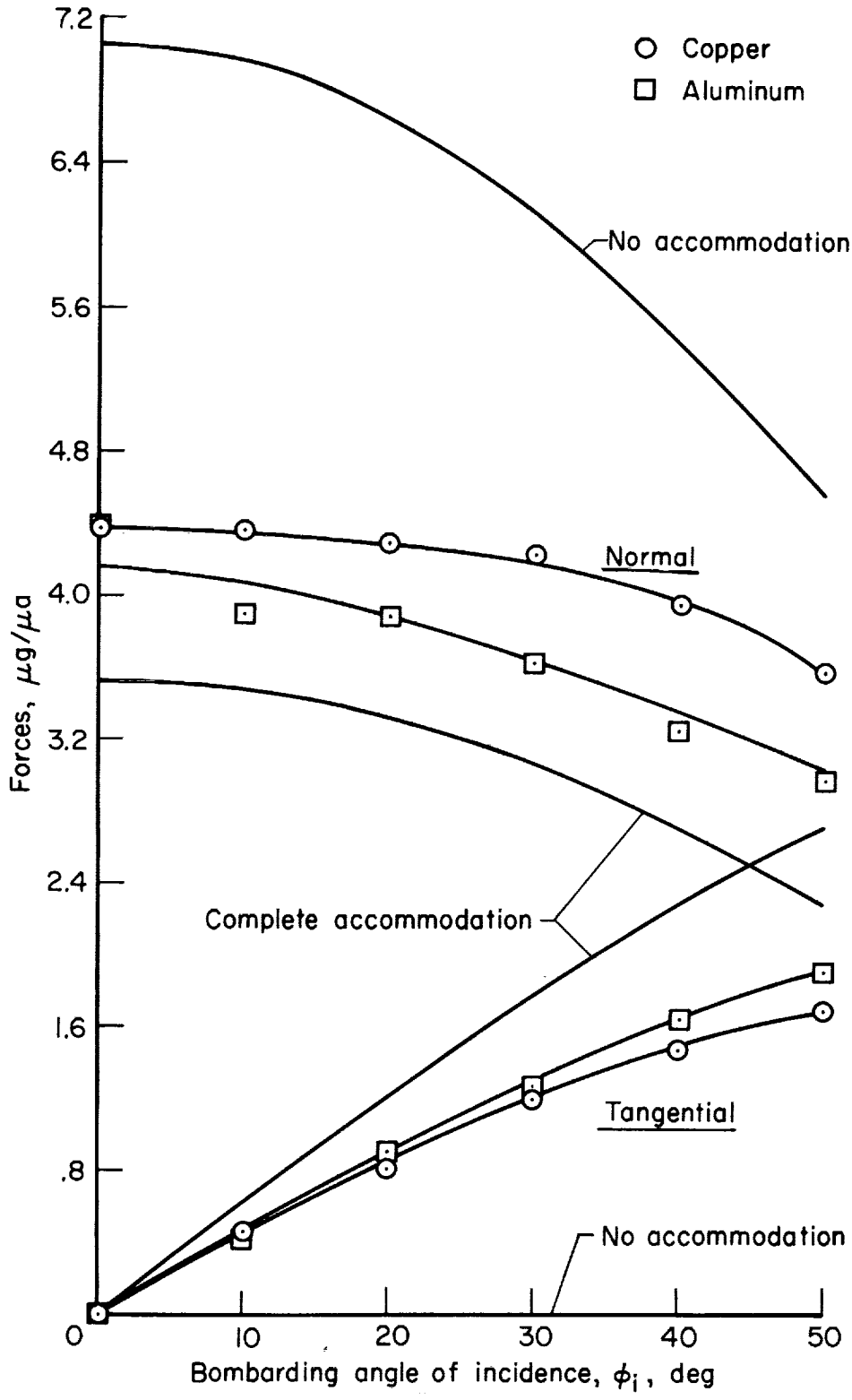

Figure 4.- Normal and tangential components of the force due to the bombardment of Cu and Al by N_2^+ at an energy of 2060 ev.

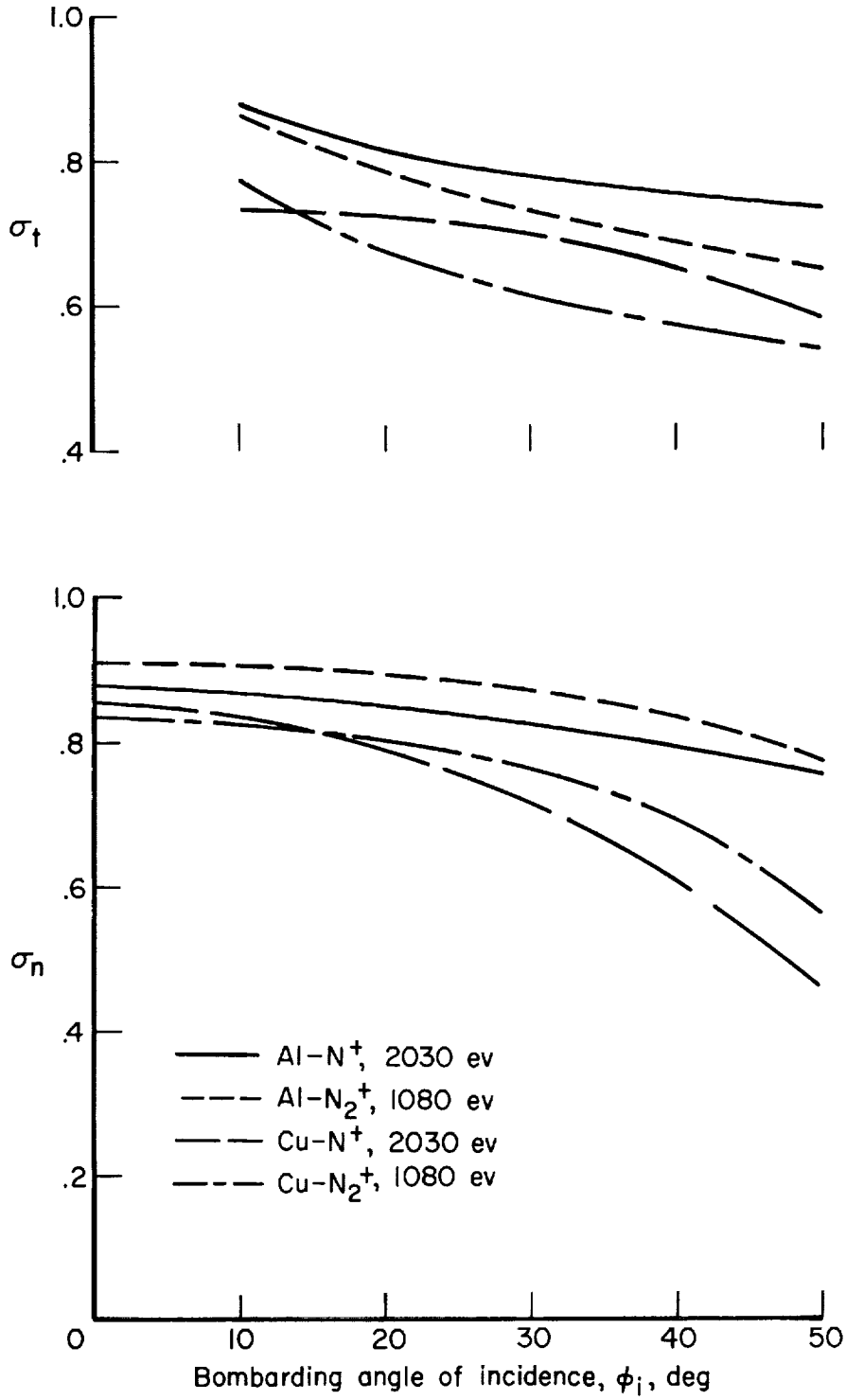

(a) Energy of N^+ = 2030 ev, energy of N_2^+ = 1080 ev.

Figure 5.- The momentum accommodation coefficients of Cu and Al bombarded by N^+ and N_2^+ as a function of angle of incidence.

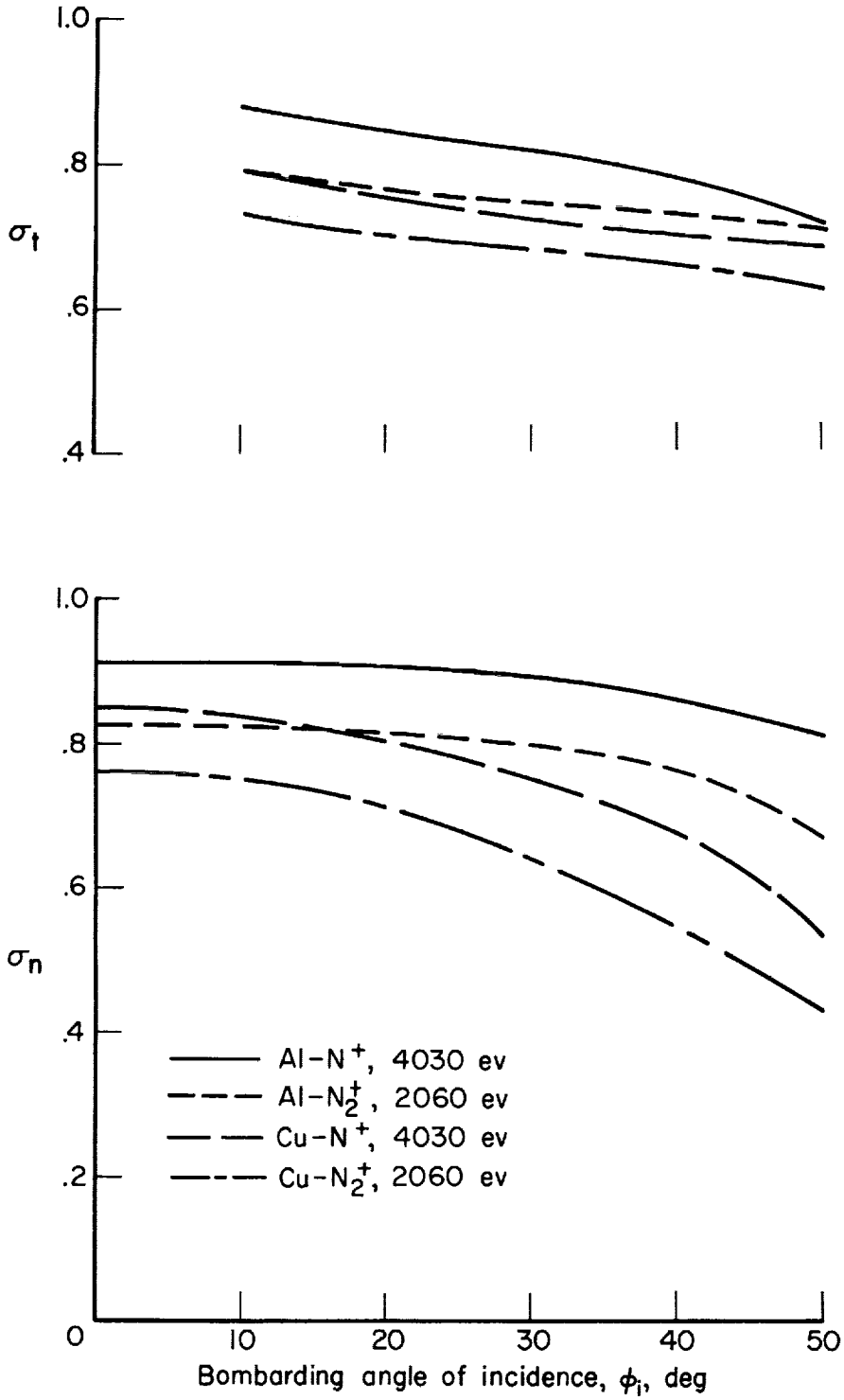

(b) Energy of N^+ = 4030 ev, energy of N_2^+ = 2060 ev.

Figure 5.- Concluded.

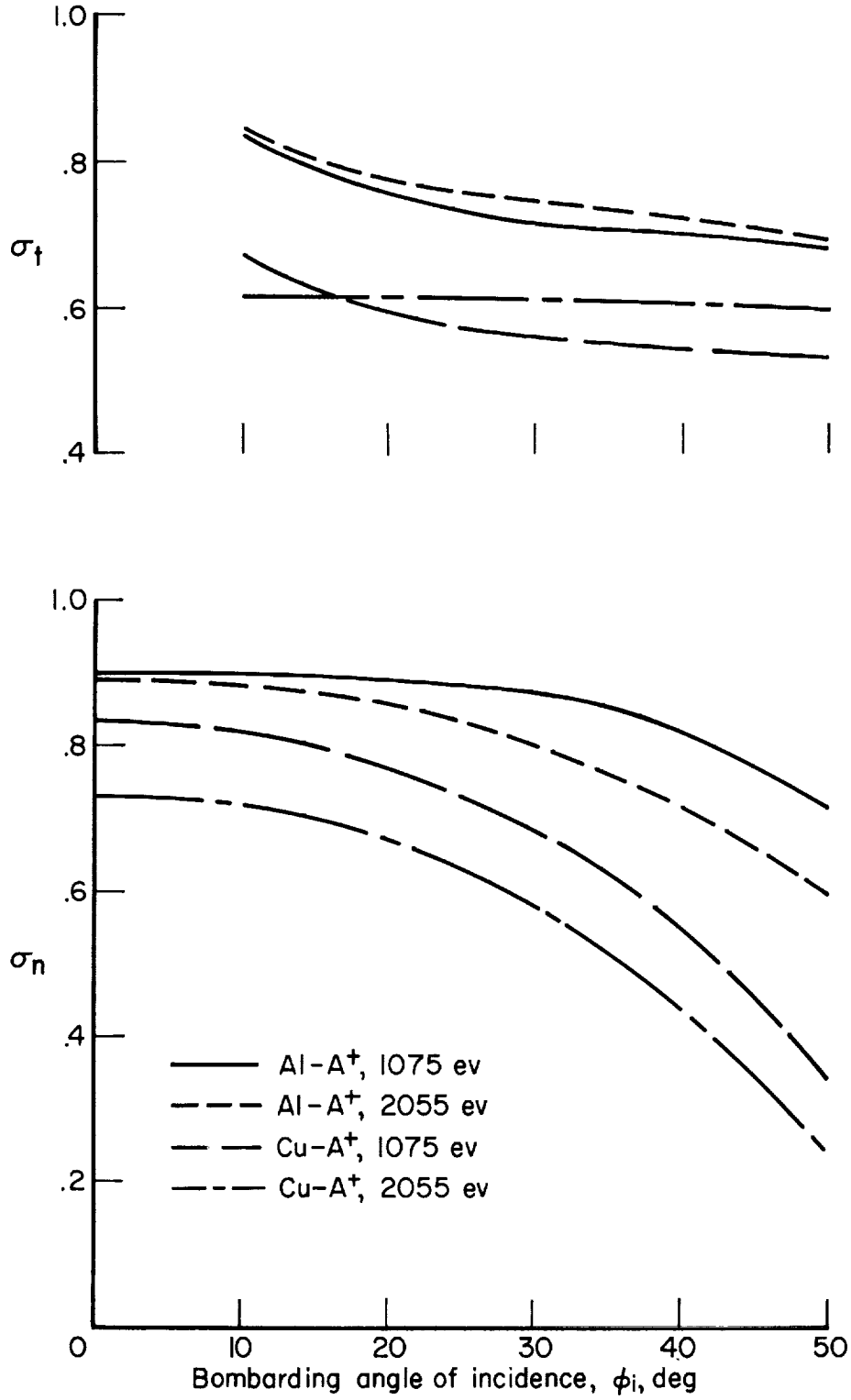

Figure 6.- The momentum accommodation coefficients of A^+ on Cu and Al as a function of angle of incidence.

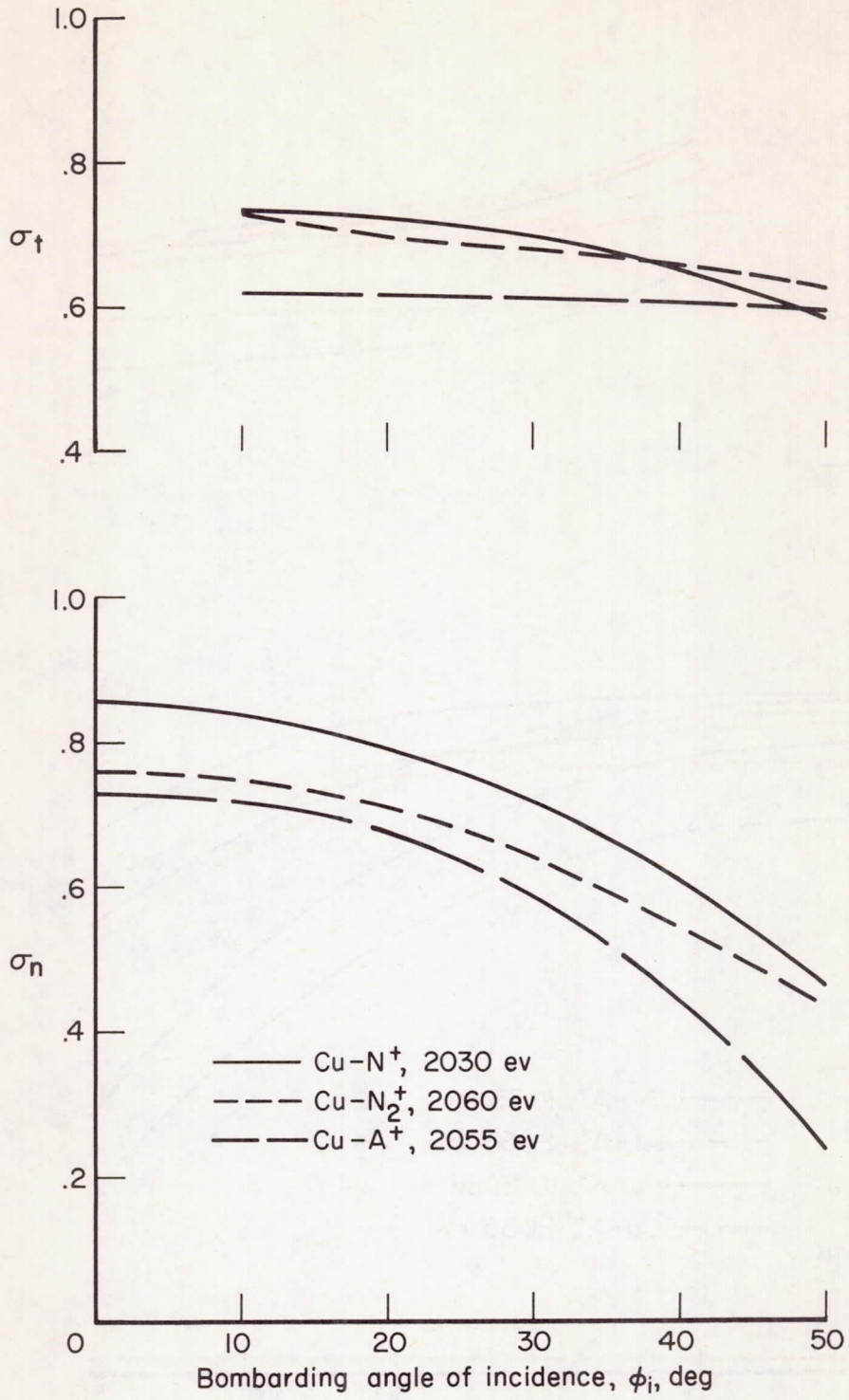

(a) N^+, N_2^+ and A^+ on Cu.

Figure 7.- Comparison of accommodation coefficients for various bombarding ions on a given surface.

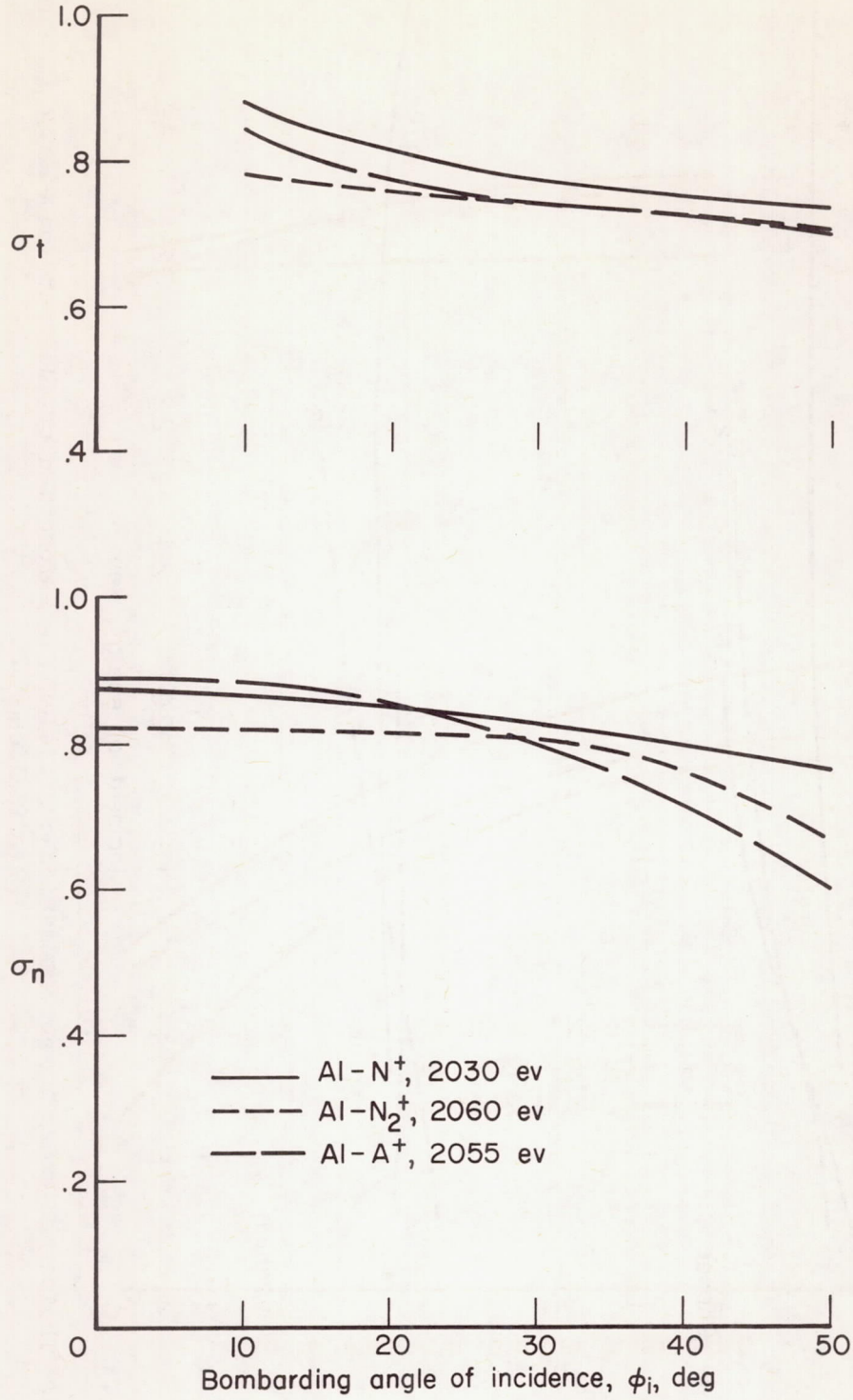

(b) N^+, N_2^+ and A^+ on Al.

Figure 7.- Concluded.

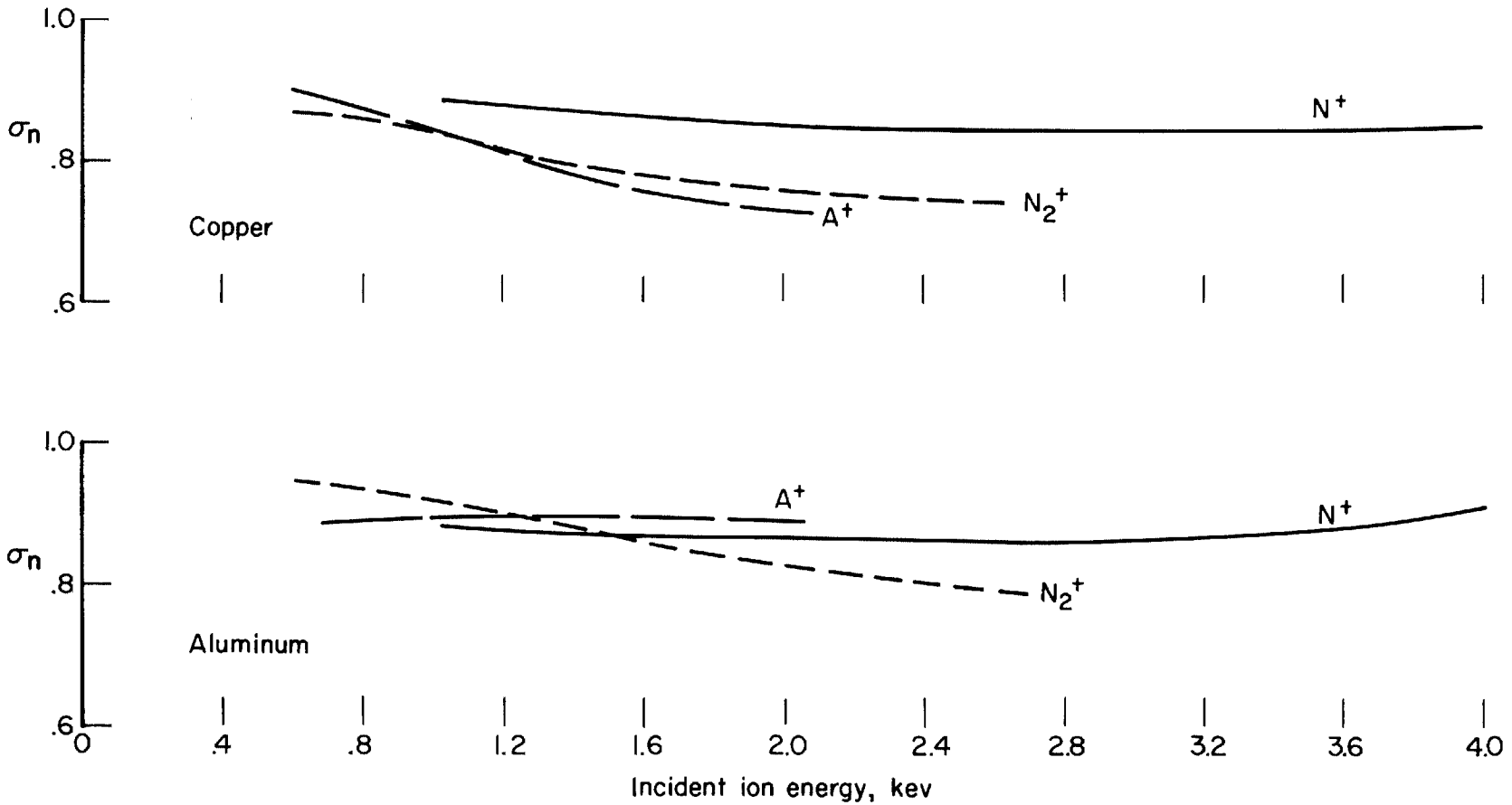

Figure 8.- The normal momentum accommodation coefficient as a function of incident ion energy at normal incidence.

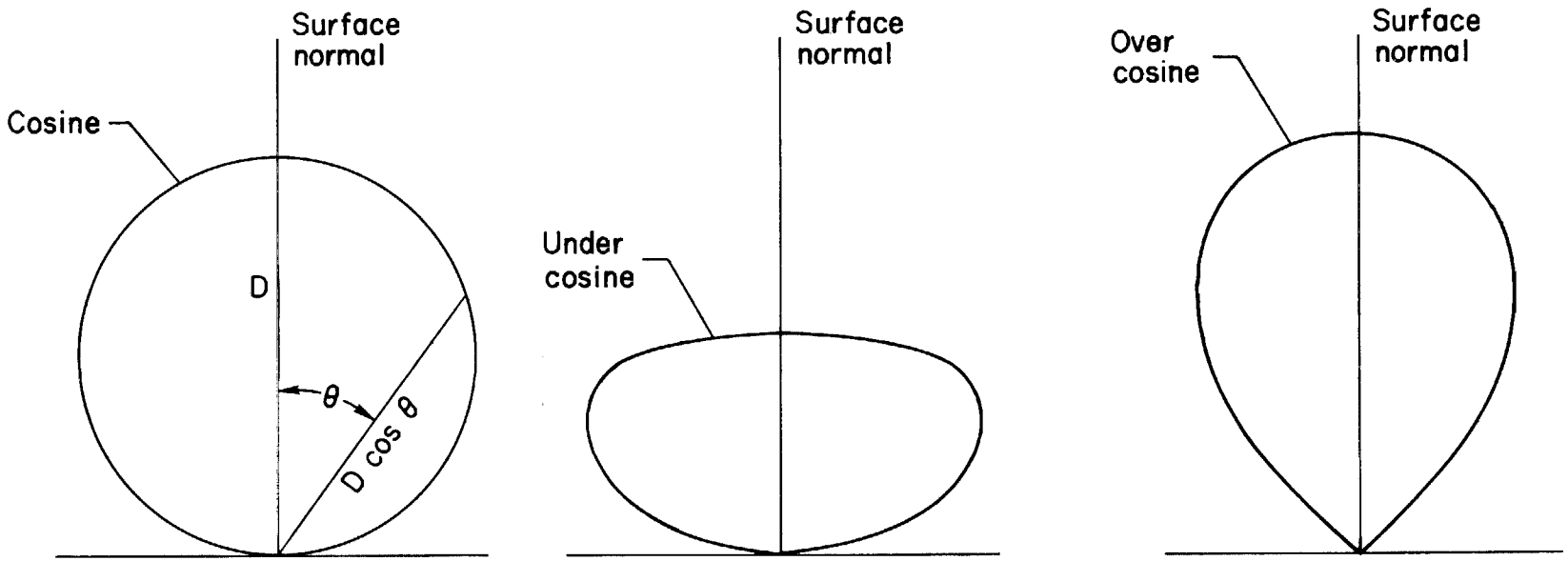

Figure 9.- Definition of cosine, under cosine, and over cosine distributions.

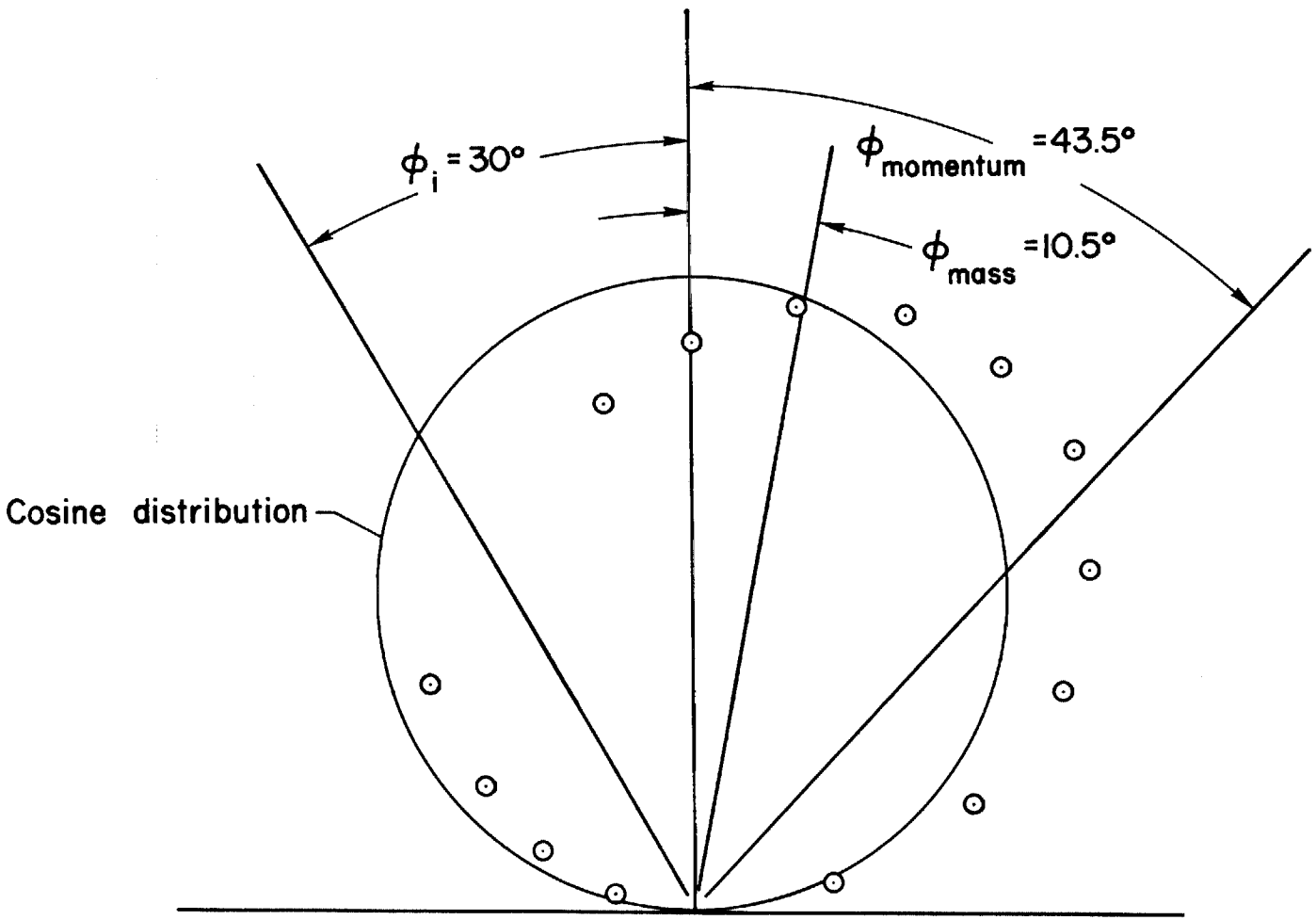

Figure 10.- Polar plot of the mass distribution of sputtered Cu resulting from N_2^+ bombardment at an energy of 1 kev; φ_i = ion angle of incidence; φ_{mass} = center of mass of sputtered material; $\varphi_{momentum}$ = computed effective direction of reflected momentum (see text).

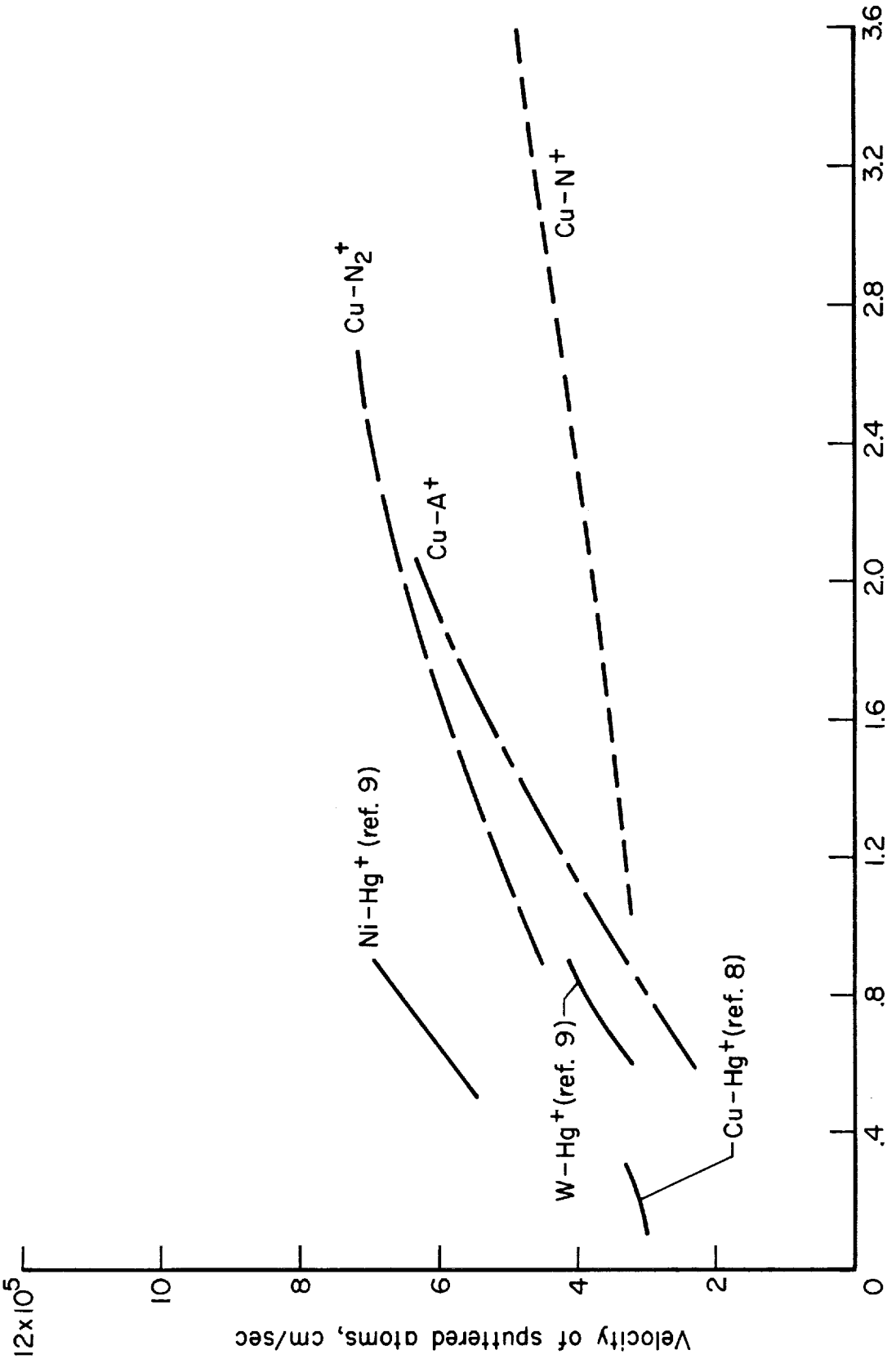

Figure 11.- The average velocities of sputtered atoms as a function of incident ion energy at normal incidence.